Architecture dependence of thermal fluctuation effects on the order–disorder transition of block copolymer melts

Ken-ichi Nakamura [*],[1], Shotaro Nishitsuji, Mikihito Takenaka [*], Makoto Ouchi, Mitsuo Sawamoto [*]

Department of Polymer Chemistry, Graduate School of Engineering, Kyoto University, Kyotodaigakukatsura Nishikyo-ku, Kyoto 615-8510, Japan

ARTICLE INFO

ABSTRACT

Small-angle X-ray scattering has done to explore the difference in the strength of the thermal fluctuation effects between A–B diblock copolymer and $(A/2)_2$–B Y-shaped copolymer. SAXS profiles for both systems in their disordered states were analyzed with the Brazovskii-type non-mean field theory by Fredrickson and Helfand. The analyses yielded Ginzburg number characterizing the strength of thermal fluctuation effects. Ginzburg number of Y-shaped copolymer is larger than that of diblock copolymer, suggesting that the strength of the thermal fluctuation effects is affected by the architecture of copolymers.

© 2008 Elsevier Ltd. All rights reserved.

1. Introduction

Binary block copolymer consists of two kinds of chemically distinct linear polymer chains, which are connected at the end of each block chain by covalent bonds. Due to the connection between the two components, binary block copolymers cause the microphase transition from homogeneous or disordered state to ordered state with Flory–Huggins segmental interaction parameter χ between the two components, instead of macrophase separation [1,2]. In ordered state, binary block copolymers exhibit a variety of unique periodic structures with long periodicity in the order of 10–100 nm such as lamella, *Fddd* [3], Gyroid, hexagonally-packed cylinder, and sphere on body center cubic lattice. Morphologies of the ordered structure have been extensively investigated and have been found to depend on volume ratio of two components and segregation power characterized by χN, where N is the polymerization index of binary block copolymers. Moreover, the morphologies also depend on the architecture of binary block copolymers. For example, Milner [4] predicted the phase diagram of A_2B Y-shaped copolymer for ordered structure shifts to B-rich region in comparison with the corresponding diblock copolymer. In disordered state, the domain structure disappears and the concentration fluctuations induced by thermal noise exist. Even in disordered state, the q-Fourier mode of the concentration fluctuations or scattering function has a peak due to the connectivity between the two components. Leibler proposed the theory on the behaviour of diblock copolymer in the disordered state and weak segregation limit of the ordered state in the context of mean field theory [5]. According to Leibler's theory, the inverse of the peak intensity of the scattering function in disordered state is proportional to the inverse of temperature and becomes zero at spinodal temperature of the order–disorder transition of diblock copolymers, if χ is inversely proportional to temperature. However, Fredrickson–Helfand [6,7] first showed that the thermal fluctuation effects affect the order–disorder transition and the concentration fluctuations in the disordered state. The thermal fluctuation effects stabilize the disordered state and shift T_{ODT} lower than the spinodal temperature estimated with the mean field theory and hence change the nature of the phase transition from second-order in the mean field theory to the weakly first-order due to thermal fluctuation effects for symmetric diblock copolymers. The effects were theoretically explored later by Fredrickson and Binder [8]. Experimentally, the effects have for the first time been illuminated by Bates et al. [9] and later by some other groups [10–12]. The strength of the thermal fluctuation effects has also been discussed and is affected by various factors. The theory by Fredrickson and Binder [8] explored that the strength of the thermal fluctuation effects is proportional to $N^{-2/3}$. Schwahn et al. have investigated the pressure dependence of the strength of the thermal fluctuation effects in diblock copolymers in terms of the Ginzburg number which will be described later [13,14]. Miyazawa et al. explored the pressure dependence of the strength of the thermal fluctuation effects in diblock copolymer solutions [15]. Similar to the architecture effects in the ordered state, we can anticipate that the concentration fluctuations in the disordered state are also affected by the architecture of binary block copolymers.

* Corresponding authors.
  E-mail address: kenichi_nakamura@mail.toagosei.co.jp (K.-ichi Nakamura).
[1] Present address: Toagosei Company Limited, Corporate Research Laboratory, 1-1 Funami-cho, Minato-ku, Nagoya, Aichi 455-0027, Japan.
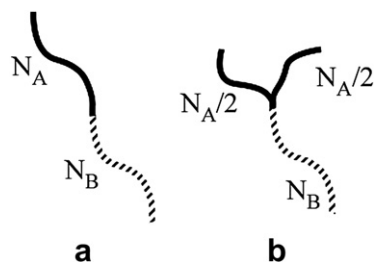
Fig. 1. Schematic picture of (a) A–B diblock copolymer and (b) $(A/2)_2$–B Y-shaped copolymer used in this study.

Thus, in this study, we shall aim to explore the architecture dependence of the thermal fluctuation effects in disordered state. To clarify the dependence, we employed A–B diblock copolymer and $(A/2)_2$–B Y-shaped copolymer which have almost identical molecular weight but different architectures as shown in Fig. 1. We measured the scattering functions of diblock copolymer and Y-shaped copolymer in their disordered state, and analyzed the strength of the thermal fluctuation effects.

We will describe the sample and the brief explanation of synthesis procedure and the detail of SAXS experiment in Section 2. In Section 3, we will show the temperature dependence of the SAXS profiles for the diblock copolymer and Y-shaped copolymers. In Section 4, we will analyse the SAXS profiles with the Brazovskii-type non-mean field theory by Fredrickson and Helfand, and explore how the difference in the architecture modifies the strength of the thermal fluctuation effects. Finally, we shall conclude our results in Section 5.

2. Experimental method

We used two kinds of block copolymer A–B type diblock copolymer and $(A/2)_2$–B Y-shaped copolymer in this experiment to explore the effects of the architecture in block copolymers on order–disorder transition behaviours. Here we used methyl methacrylate (MMA) and isobutyl vinyl ether (IBVE) denoted as A and B components, respectively.

A–B type diblock copolymer was synthesized by difunctional initiator (R_1C_1-Init) with an initiating point for living cationic polymerization and an initiating point for radical polymerization on 1-, 3-position of benzene ring. First we employed R_1C_1-Init for living cationic polymerization of IBVE with $SnCl_4$ as a catalyst at $-78\,^{\circ}C$ in toluene. Then, the resultant poly(IBVE) bearing radical-initiating points at the terminal was used as a macroinitiator for $Ru(Ind)Cl(PPh_3)_2$-catalyzed living radical polymerization of MMA at $80\,^{\circ}C$ in toluene.

$(A/2)_2$–B type Y-shaped copolymer was synthesized by trifunctional initiator (R_2C_1-Init) with an initiating point for living cationic polymerization and two initiating points for radical polymerization on 1-, 3-, 5-position of benzene ring. Living cationic polymerization and living radical polymerization were done with the same method for diblock copolymer. The obtained block copolymers were well controlled with narrow molecular weight distribution ($M_w/M_n \sim 1.1$) without forming respective homopolymers as characterized by SEC/^{1}H NMR analyses (Table 1). According to the cleavage experiment of the Y-shaped copolymer, the A-arms exhibited unimodal SEC curves, whose molecular weight was in good

agreement with the calculated values. This result supports that each A-arm in the Y-shaped copolymer owns the same average chain length (degree of polymerization). The details of the synthetic procedure of the block copolymers are described elsewhere [16].

The block copolymer samples were dissolved into 10 wt% dichloromethane solution and evaporating the solvent slowly at room temperature. The obtained film specimens of the block copolymers were further dried in a vacuum oven at $60\,^{\circ}C$.

We measured SAXS profiles *in situ* at each temperature with a SAXS apparatus consisting of a 12 kW rotating-anode X-ray generator, a graphite crystal for monochromatizing incident beam, a 1.5 m camera, and a one-dimensional position sensitive proportional counter [17]. Cu-Kα radiation having wavelength $\lambda = 0.154$ nm was used for incident beam. The sample was set in an evacuated chamber to reduce possible thermal degradation and the temperature of the sample in the chamber was controlled with accuracy of ± 0.03 K.

We measured the SAXS profiles during the cooling processes. Before the SAXS measurement for 30 min at each temperature, we annealed the samples at each temperature for 30 min to attain the equilibrium state of the samples at measured temperatures.
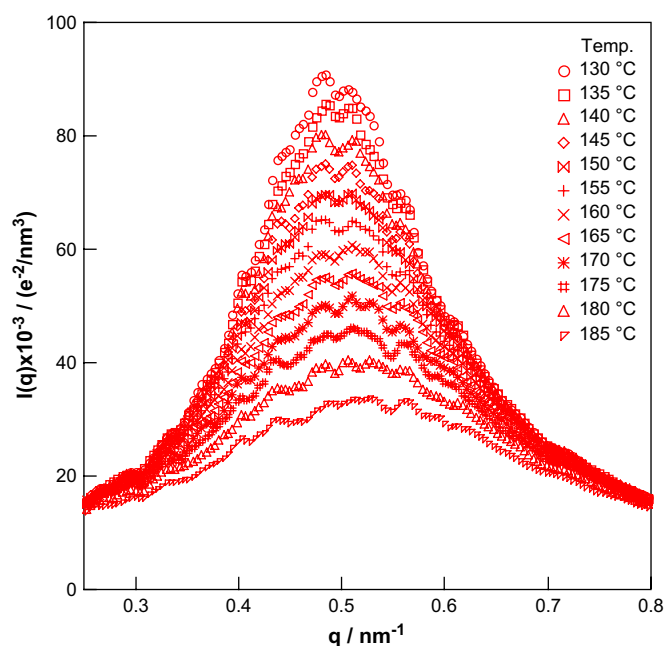
The obtained SAXS profiles were corrected for absorption by samples, air scattering and thermal diffuse scattering as described elsewhere [17b]. The SAXS profiles were further corrected for slit-width and slit-height smearing [17,18]. The absolute intensity was obtained with the nickel foil method.

3. Results

Fig. 2 shows the changes in the scattering intensity $I(q)$ for the diblock copolymer with temperature during the cooling process. Here q is the magnitude of the scattering vector defined by

$$q = \left(\frac{4\pi}{\lambda}\right) \sin \theta \tag{1}$$

with θ being the scattering angle. The scattering intensity increases with decreasing temperature and the peak position of the scattering intensity shifts toward smaller q-region with decreasing temperature. We did not find any discontinuous change in the

Table 1
Characteristics of diblock and Y-shaped copolymers used in this study

Code	$M_w \times 10^{-4}$	M_w/M_n	f_{PMMA}
Diblock	1.08	1.07	16.7
Y-shaped	1.38	1.07	17.3

f_{PMMA}: Volume fraction of PMMA.

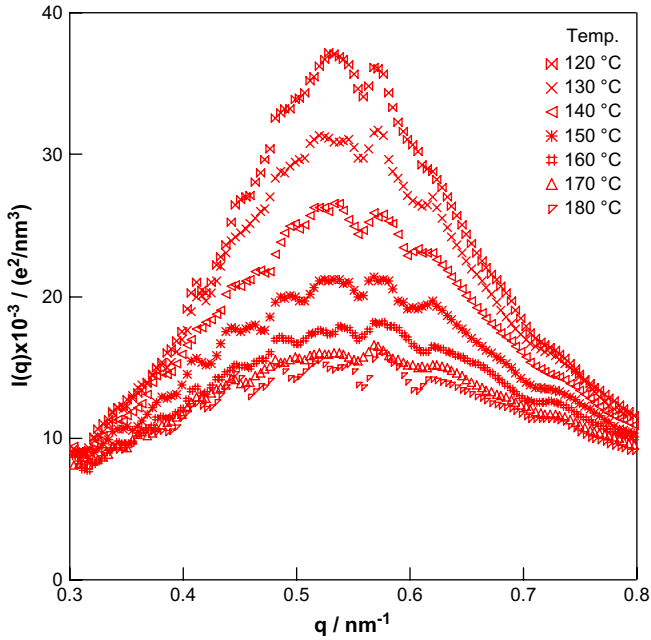**Fig. 2.** Temperature dependence of the scattering intensity $I(q)$ of diblock copolymer as a function of q.

Fig. 3. Temperature dependence of the scattering intensity $I(q)$ of Y-shaped copolymer as a function of q.

Fig. 4. Inverse of the peak intensity $I(q)^{-1}$ plotted as a function of inverse of absolute temperature T^{-1} for diblock copolymer and Y-shaped copolymer.

scattering intensity with decreasing temperature and the width of the peak in the scattering intensity is relatively broad at observed temperature range, suggesting that the diblock copolymer is in the disordered state at the temperature range covered in this study.

Fig. 3 shows the change in the scattering intensity $I(q)$ for the Y-shaped copolymer with temperature during the cooling process. Similar tendency as observed in the diblock copolymer can be found in the change in the scattering intensity of Y-shaped copolymer: the increase of the scattering intensity and the shift of the peak position toward smaller q with decreasing temperature. Since the change in the scattering intensity does not show the discontinuity and has the relatively broad peak width as well as the case in the diblock copolymer melt, the Y-shaped copolymer melt is also in the disordered state. We will analyze the SAXS profiles shown in Figs. 2 and 3 in the next section.

4. Analyses and discussion

According to the mean field theory by Leibler [5], the peak scattering intensity $I(q_m)$ is proportional to T^{-1} and diverge at the spinodal temperature (T_S) as expressed by

$$I(q_m)^{-1} \propto 2(\chi_S - \chi) \propto \frac{1}{T_S} - \frac{1}{T} \qquad (2)$$

We estimated $I(q_m)$ by fitting SAXS profiles with Gaussian function. Fig. 4 shows $I(q_m)^{-1}$ plotted against inverse of temperature T^{-1} for diblock and Y-shaped block copolymers. Contrary to the prediction of the mean field theory, the plots of $I(q_m)^{-1}$ *vs.* T^{-1} for both the systems curve downwards, which indicates that the order-disorder transition (ODT) behaviours of diblock and Y-shaped block copolymers are affected by thermal fluctuations. We can estimate the characteristic length $D = 2\pi/q_m$ from the fitting. D of both the copolymers increases with decreasing temperature, indicating that the chain stretching occurs due to the thermal fluctuation effects as observed previously [9].

Fredrickson and Helfand [6,7] considered the thermal fluctuation effects on the free energy functional of block copolymers and proposed the structure factor $F(q)$, which is proportional to $I(q)$, in the disordered state for binary block copolymers:
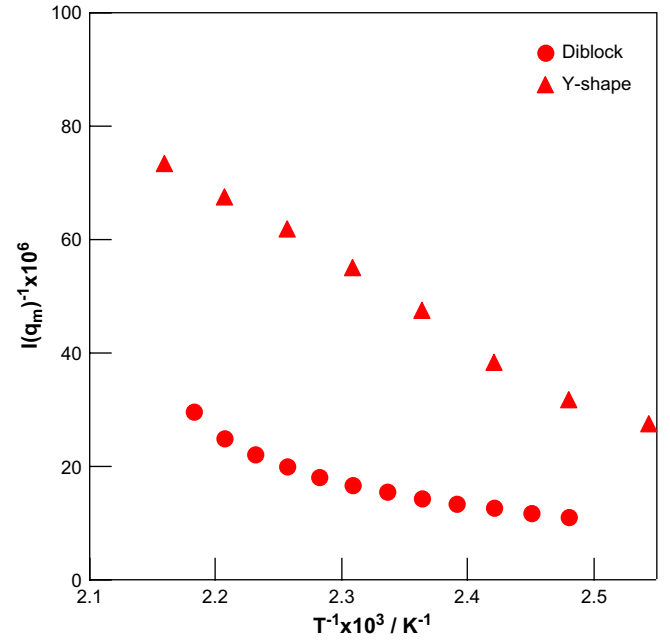
$$F(q)^{-1} = \frac{S(q)}{W(q)} - 2\chi_{\mathrm{ren}} = kI(q)^{-1} \qquad (3)$$

with

$$S(q) = S_{\mathrm{AA}}(q) + 2S_{\mathrm{AB}}(q) + S_{\mathrm{BB}}(q) \qquad (4)$$

$$W(q) = S_{\mathrm{AA}}(q)S_{\mathrm{BB}}(q) - 2[S_{\mathrm{AB}}(q)]^2 \qquad (5)$$

where $S_{ij}(q)$ (i,j = A or B) is the q-Fourier component of the concentration correlation function between i and j monomers [19] and depends on the architecture of binary block copolymers. The details of $S(q)$ and $W(q)$ for diblock copolymer and Y-shaped copolymer are described in Appendix. Since polydispersity in molecular weight and an asymmetry in segmental volume affect the structure factor significantly [19], we considered the effects of the polydispersity and the asymmetry on $F(q)$. k is the contrast factor between the two components for the scattering. χ_{ren} is the renormalized Flory–Huggins interaction parameter. The renormalized χ_{ren} includes the thermal fluctuation effects and is related to "true" Flory–Huggins interaction parameter χ by

$$\chi_{\mathrm{ren}} = \chi - \frac{G_i}{r_c^{3/2}} \sqrt{F(q_m)} \qquad (6)$$

where G_i is Ginzburg number and characterizes the strength of thermal fluctuation effects. r_c is the effective total degree of polymerization and is defined as $r_c = (v_A/v_0)N_A + (v_B/v_0)N_B$; v_k is the molar volume of k-monomer and N_k is the number-average degree of polymerization of k-block chain. v_0 is the reference volume defined as $v_0 = (v_A v_B)^{0.5}$. As expressed in Eq. (6), χ_{ren} becomes smaller than χ due to the second term on the right side including the thermal fluctuation effects, though χ_{ren} corresponds to χ parameter in the mean field theory. χ is usually expressed as

$$\chi = \alpha + \frac{\beta}{T} \qquad (7)$$

where α and β are, respectively, entropic and enthalpic contributions. From Eqs. (6) and (7), $F(q_m)^{-1}$ is given by

$$F(q_{\mathrm{m}})^{-1} = \frac{G_i^2}{r_c^3}(\chi - \chi_{\mathrm{ren}})^{-2} = \frac{G_i^2}{r_c^3}\left(\alpha + \frac{\beta}{T} - \chi_{\mathrm{ren}}\right)^{-2} \qquad (8)$$

To compare the strength of the thermal fluctuation effects in both the systems, we obtained temperature dependence of $F(q_{\mathrm{m}})^{-1}$ and χ_{ren} by fitting SAXS profiles with Eqs. (3)–(5) and then G_i, α and β are obtained by fitting temperature dependence of $F(q_{\mathrm{m}})^{-1}$ and χ_{ren} with Eq. (8).

First, we estimated $F(q_{\mathrm{m}})^{-1}$ and χ_{ren} from fitting the scattering intensity with Eqs. (3)–(5). Fig. 5 shows the fitting results of the scattering intensity for both the systems. We can fit the data with Eqs. (3)–(5) nicely and estimate the temperature dependencies of $F(q_{\mathrm{m}})$ and χ_{ren}. Fig. 6 shows the plots of $F(q_{\mathrm{m}})^{-1}$ vs. T^{-1} in the disordered states for the diblock and Y-shaped copolymers. The plots for both the systems have curvature, indicating that the thermal fluctuations affect the ODT behaviours of both the systems. This fact also can be seen in the plots of χ_{ren} vs. T^{-1} or Fig. 7. Both the plots do not show linear relationship but have curvature, indicating that the thermal fluctuation effects affect the temperature dependence of χ_{ren}. We can also estimate the statistical segment length of each component. The averaged statistical segment length at 100 °C is 1.08 nm and is larger than the statistical segment length of PMMA,
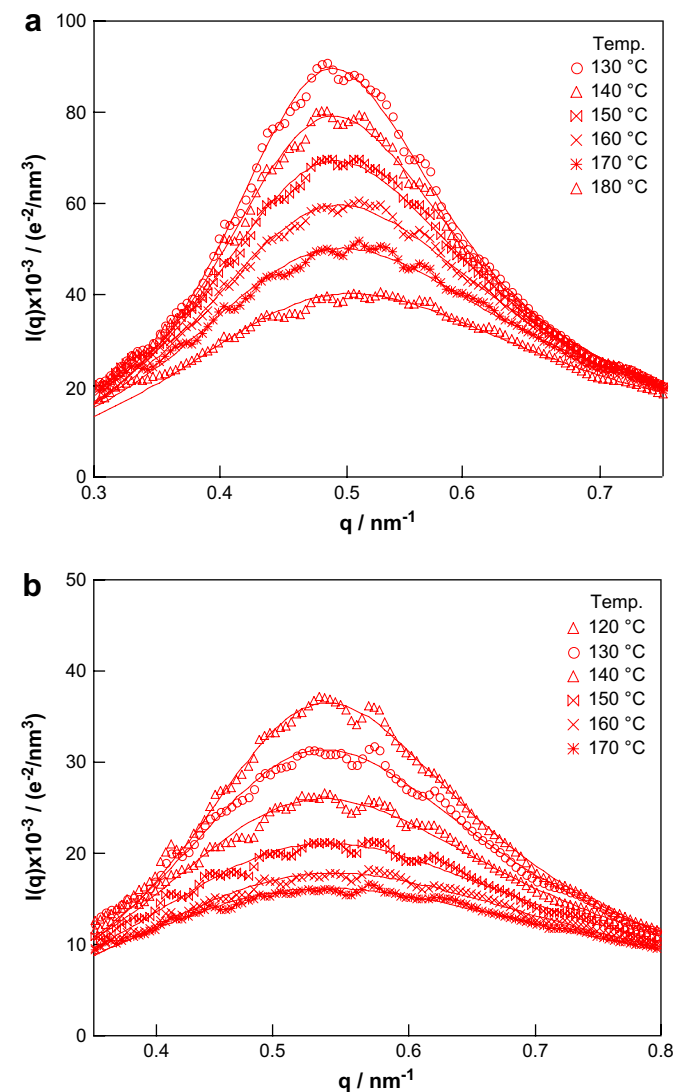

Fig. 6. Inverse of the structure factor $F(q_{\mathrm{m}})^{-1}$ plotted as a function of inverse of absolute temperature T^{-1} for diblock copolymer and Y-shaped copolymer.

0.745 nm, estimated from the dilute PMMA solution at θ condition [20], suggesting that the chain stretching occurs near ODT.

To evaluate the strength of the thermal fluctuation effects in both the systems, we estimated Ginzburg number for both the systems by fitting the data by Eq. (8). The fitting results are shown in Fig. 6 as solid lines. Eq. (8) can well describe the behaviours of the temperature dependencies of $F(q_{\mathrm{m}})$ and the fitting yielded G_i, α, and β. The values of G_i, α, and β are listed in Table 2. G_i for the Y-shaped copolymer is slightly larger than that for the diblock copolymer, indicating that the strength of the thermal fluctuation effects of the Y-shaped copolymer is more than that of the diblock copolymer.

In the context of the mean field theory, a monomer A is assumed to be surrounded by monomer B with the probability being the volume fraction of monomer B. However, near order–disorder

Fig. 5. Fitting results of the scattering intensity data with Eqs. (3)–(5) given by Fredrickson and Helfand for (a) diblock copolymer and (b) Y-shaped copolymer. The detail of the fitting functions is given in Appendix.
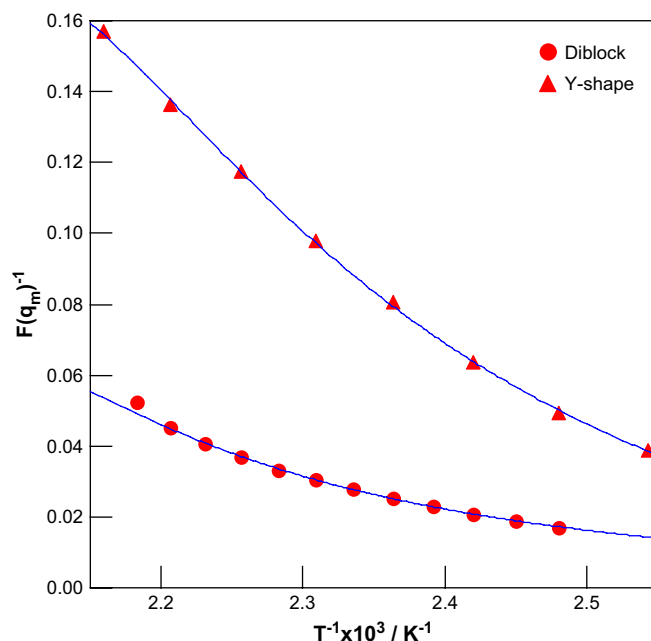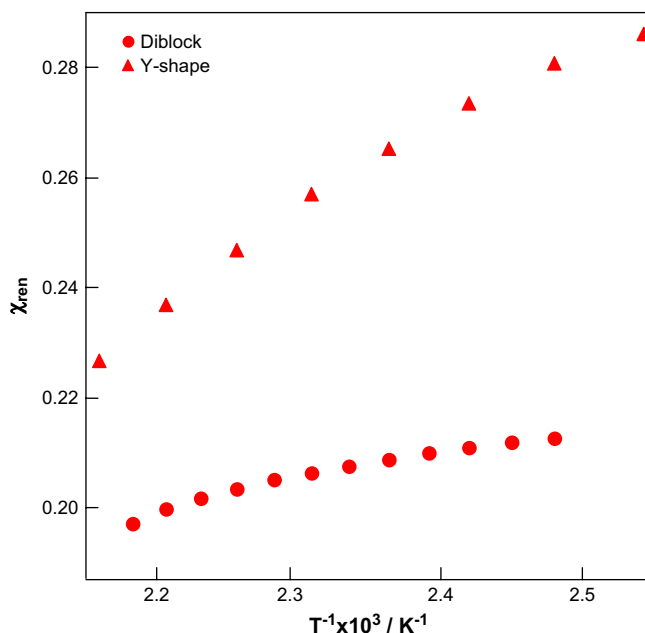

Fig. 7. Renormalized χ_{ren} is plotted as inverse of absolute temperature T^{-1}.

Table 2
G_i, α, and β for diblock copolymer and Y-shaped copolymer

Code	G_i	α	β
Diblock	24.3 ± 5.9	-0.381 ± 0.141	319.0 ± 80.1
Y-shaped	28.1 ± 8.5	-0.356 ± 0.016	294.9 ± 9.3

transition, the concentration fluctuation rather enhances the stability of the disordered state and hence apparently miscibility is enhanced even though the segmental interaction is above that at spinodal point. Thus the assumption of the mean field theory is not valid and the effective interaction between A and B expressed by χ_{ren} decreases. In our study, we found that the strength of the thermal fluctuation effects of the Y-shaped copolymer is more than that of the diblock copolymer. The chain architecture affects the strength of fluctuation effects in terms of two factors. One is the enhancement of contact probability between A and B due to the chain architecture of Y-shape. In comparison with the architecture of diblock copolymer, the probability of the contact between A and B monomers seems to be enhanced by the architecture where two of half-length of A polymers are connected to B polymer at each end as shown in Fig. 1 and reduce the effects of the thermal fluctuations. The other is steric hindrance around the junction point. The steric hindrance prevents the interpenetration of other polymer chains around the junction point. This steric hindrance enhances the strength of the effects of the thermal fluctuations and has opposite effects to the former factor. The experimental results suggest that the steric hindrance is more effective than the former factor so that the Ginzburg number of the Y-shaped copolymer becomes larger than that of the diblock copolymer.

Fig. 8 shows the temperature dependence of χ expressed as $\chi = \alpha + \beta/T$ for both the systems. At observed region, χ for Y-shaped copolymer is smaller than that for diblock copolymer. The difference in χ is due to the effects of the steric hindrance of Y-shaped copolymer. The steric hindrance reduces the contact between A and B. Similar behaviour is observed in the arm number dependence of χ of star block copolymers (A–B)$_n$, where n is arm number of the star block copolymers. According to Ijichi et al. [21,22], χ of star block copolymers at a given temperature decreases with arm number because of the steric hindrance. This fact in the arm number dependence of χ of star block copolymers is consistent with our result.
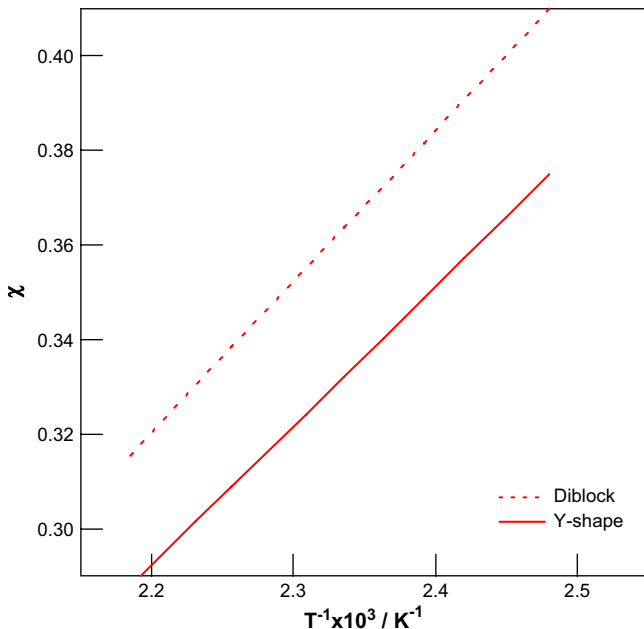
Fig. 8. True χ is plotted as inverse of absolute temperature T^{-1}.

5. Conclusion

We have investigated the temperature dependencies of the concentration fluctuations for A–B diblock copolymer and (A/2)$_2$–B Y-shaped copolymer in their disordered state by using SAXS. The plots of $I(q_m)^{-1}$ vs. T^{-1} for both the systems show downward curvature, suggesting that the thermal fluctuation effects influence the behaviours of the concentration fluctuations. We analyzed SAXS profiles for both the systems in their disordered state with the Brazovskii-type non-mean field theory by Fredrickson and Helfand and the analyses yielded Ginzburg number characterizing the strength of thermal fluctuation effects. Ginzburg number of Y-shaped copolymer is larger than that of diblock copolymer, suggesting that the strength of the thermal fluctuation effects in diblock copolymer is more than that in Y-shaped copolymer. There are the following reciprocal factors affecting the fluctuation effects in terms of architectures: (i) the enhancement of contact probability between A and B caused by Y-shaped copolymer and (ii) the steric hindrance around branch point of Y-shaped copolymer. We found that factor (ii) is more effective than factor (i), and that the strength of the thermal fluctuation effects are affected by the architecture of binary block copolymers.

Appendix

Here we briefly describe the structure factor $F(q)$ from the disordered melt of A–B diblock copolymer and Y-shaped copolymer with a polydispersity in molecular weight and an asymmetry in segmental volume. As described in Eq. (3), $F(q)$ is given by

$$F(q) = [S(q)/W(q) - 2\chi_{\text{ren}}]^{-1} \tag{A1}$$

with

$$S(q) = S_{AA}(q) + S_{AB}(q) + S_{BB}(q) \tag{A2}$$

$$W(q) = S_{AA}(q)S_{BB}(q) - [S_{AB}(q)]^2 \tag{A3}$$

For diblock copolymer, $S_{AA}(q)$, $S_{BB}(q)$, and $S_{AB}(q)$ are expressed by

$$S_{AA}(q) = r_{c,n}f_{A,n}^2 g_{A,n}^{(2)}(q) \tag{A4}$$

$$S_{BB}(q) = r_{c,n}f_{B,n}^2 g_{B,n}^{(2)}(q) \tag{A5}$$

and

$$S_{AB}(q) = r_{c,n}f_{A,n}f_{B,n}g_{A,n}^{(1)}(q)g_{B,n}^{(2)}(q) \tag{A6}$$

Here $r_{c,n}$ and v_0 are given by

$$r_{c,n} = (v_A/v_0)N_{A,n} + (v_B/v_0)N_{B,n} \tag{A7}$$

and

$$v_0 = \sqrt{v_A v_B} \tag{A8}$$

where v_K is the molecular volume of K-th monomer (K = A or B), and $N_{K,n}$ is number-average degree of polymerization of K-th block chain. $g_{K,n}^{(1)}(q)$ and $g_{K,n}^{(2)}(q)$ are expressed by

$$g_{K,n}^{(1)}(q) = \frac{1}{x_{K,n}}\left\{1 - [x_{K,n}(\lambda_K - 1) + 1]^{-(\lambda_K - 1)^{-1}}\right\} \tag{A9}$$

$$g_{K,n}^{(2)} = \frac{2}{x_{K,n}^2}\left\{-1 + x_{K,n} + [x_{K,n}(\lambda_K - 1) + 1]^{-(\lambda_K - 1)^{-1}}\right\} \tag{A10}$$

with

$$x_{K,n} \equiv \left(N_{K,n}b_K^2/6\right)q^2 \tag{A11}$$

$$\lambda_K = N_{K,w}/N_{K,n} \tag{A12}$$

$$f_{K,n} = N_{K,n}v_K/(N_{A,n}v_A + N_{B,n}v_B) \tag{A13}$$

b_K in Eq. (A11) is statistical segment length of K-th chain, and $N_{K,w}$ in Eq. (A12) is weight average degree of polymerization of the K-th chain. If we assumed $\lambda = \lambda_A = \lambda_B$, λ can be estimated from M_w/M_n for the whole diblock copolymer chain,

$$\lambda = \left[(M_w/M_n - 1)/\left(w_A^2 + w_B^2\right)\right] + 1 \tag{A14}$$

where $w_A = 1 - w_B$ is weight fraction of the A block chain in A–B diblock copolymer.

For A_2B Y-shaped copolymer, $S_{AA}(q)$, $S_{BB}(q)$, and $S_{AB}(q)$ are expressed by

$$S_{AA}(q) = r_{c,n}f_{A,n}^2 g_{A,n}^{(2)}(q) \tag{A15}$$

$$S_{BB}(q) = r_{c,n}f_{B,n}^2 g_{B,n}^{(2)}(q) \tag{A16}$$

and

$$S_{AB}(q) = r_{c,n}f_{A1,n}f_{B,n}g_{A1,n}^{(1)}(q)g_{B,n}^{(2)}(q) + r_{c,n}f_{A2,n}f_{B,n}g_{A2,n}^{(1)}(q)g_{B,n}^{(2)}(q) \tag{A17}$$

Here A1 and A2 denote each arm of A-component in Y-shaped copolymer and A represents total of A1 and A2. Thus, $N_{A,n}$ and $f_{A,n}$ are given by

$$N_{A,n} = N_{A1,n} + N_{A2,n} \tag{A18}$$

$$f_{A,n} = f_{A1,n} + f_{A2,n} \tag{A19}$$

For $r_{c,n}$, v_0, $g_{K,n}^{(1)}(q)$, and $g_{K,n}^{(2)}(q)$, we can use Eqs. (A7)–(A13) for Y-shaped copolymer. If we assume $\lambda = \lambda_{A1} = \lambda_{A2} = \lambda_B$, Eq. (A14) is available for Y-shaped copolymer.

References

[1] Bates FS, Fredrickson GH. Annual Review of Physical Chemistry 1990;41:525.
[2] Hashimoto T. Thermoplastic elastomers. In: Legge NR, Hlden G, Schroeder HE, editors. Vienna: Hanser; 1987. p. 349.
[3] Takenaka M, Wakada T, Akasaka S, Nishitsuji S, Saijo K, Shimizu H, et al. Macromolecules 2007;40:4399.
[4] Milner ST. Macromolecules 1994;27:2333.
[5] Leibler L. Macromolecules 1980;13:1602.
[6] Frecrickson GH, Helfand E. Journal of Chemical Physics 1987;87:697.
[7] Fredrickson GH, Helfand E. Journal of Chemical Physics 1988;89:5890.
[8] Fredrickson GH, Binder K. Journal of Chemical Physics 1989;91:7265.
[9] Bates FS, Rosedale JH, Fredrickson GH. Journal of Chemical Physics 1990;92:6255.
[10] Hashimoto T, Ogawa T, Han CD. Journal of the Physical Society of Japan 1994; 63:2206.
[11] Sakamoto N, Hashimoto T. Macromolecules 1995;28:6825.
[12] Stuhn B, Mutter R, Albrecht T. Europhysics Letters 1992;18:427.
[13] Schwahn D, Frielinghaus H, Mortensen K, Almdal K. Physical Review Letters 1996;77:3153.
[14] Schwahn D, Schmackers T, Mortensen K. Physical Review E 1995;52:R1288.
[15] Miyazawa M, Takenaka M, Miyajima T, Hashimoto T. Journal of Applied Crystallography 2003;36:656.
[16] Nakamura K, Ouchi M, Sawamoto M, Nishitsuji S, Takenaka M. Polymer Pre-print 2007;56(2):1B19.
[17] (a) Hashimoto T, Suehiro S, Shibayama M, Saijo K, Kawai H. Polymer Journal 1981;13:501;
(b) Hashimoto T, Shibayama M, Kawai H. Macromolecules 1980;13:1237.
[18] Suehiro S, Saijo K, Ohta Y, Hashimoto T. Analytica Chimica Acta 1986;189:41.
[19] Sakurai S, Mori K, Okawara A, Kimishima K, Hashimoto T. Macromolecules 1992;25:2679.
[20] Polymer handbook. In: Brundrup J, Immergut EH, editors. New York: John Wiley and Sons; 1989.
[21] Hashimoto T, Ijichi Y, Fetters LJ. Journal of Chemical Physics 1988;89:2463.
[22] Ijichi Y, Hashimoto T, Fetters LJ. Macromolecules 1989;22:2817.